A HIGHLY DENSE NANONEEDLE ARRAY FOR INTRACELLULAR GENE DELIVERY

Seung-Joon Paik[1], Seonhee Park[2], Vladimir Zarnitsyn[2], Seungkeun Choi[1], Xin Dong Guo[2], Mark R. Prausnitz[2], and Mark G. Allen[1,2]*
[1]School of Electrical and Computer Engineering
[2]School of Chemical and Biomolecular Engineering
Georgia Institute of Technology, Atlanta, Georgia, USA

ABSTRACT

We present a dense needle array with sharp nano-tips for intracellular gene and drug delivery, with the ultimate goal of gene correction in a high throughput manner. The nanoneedles are fabricated using isotropic dry etching of silicon, followed by anisotropic dry etching and thermal-oxidation-based tip sharpening. The nanoneedle density is as large as 10^6 needles per square centimeter. *In-vitro* intracellular delivery tests demonstrated that the nanoneedle array can effectively deliver molecular probes into cells without causing significant cell death from cell membrane penetration. Uptake of molecular probes by up to 34% of cells after nanoneedle treatment was observed.

INTRODUCTION

Investigation into cellular functions requires the ability to apply specific and controlled treatment to cells. Such treatment includes the delivery of biological effectors across cell membranes using various approaches such as chemical, mechanical or electrical perturbations to cells [1]. In addition to investigation, gene correction represents an active treatment in which genetic diseases and cancer may be treated by correcting the causative mutations in the genetic code. Sickle cell disease is the most common inherited blood disorder caused by a mutation of a single nucleotide of a gene. The disease causes hemoglobin-containing red blood cells to tend to deform, clump and break apart, resulting in clogged blood vessels and causing severe pain, serious infection and organ damage. Bone marrow transplantation, the only permanent cure for the disease, has the undesirable limitation of donor compatibility. Research has shown that transforming defective blood-forming cells into normal ones by inserting corrective genes can alleviate the disease [2].

Several techniques currently exist for gene correction, including biological methods or physical injection of therapeutic agents into cells. Physical methods such as conventional microinjection typically use glass microcapillaries; however, these techniques have relatively low throughput due to the time-consuming operation of targeting individual cell nuclei [1]. A micron-scale microcapillary array, made of SiO_2, was previously demonstrated for fluorescent dye injection [3] and DNA injection [4] to plant cells. In this paper we propose a silicon nanoneedle array with needle tip diameters in tens of nanometers, enabling pinpoint injection of individual cells in a high throughput manner without causing cell death by puncture (Fig. 1).

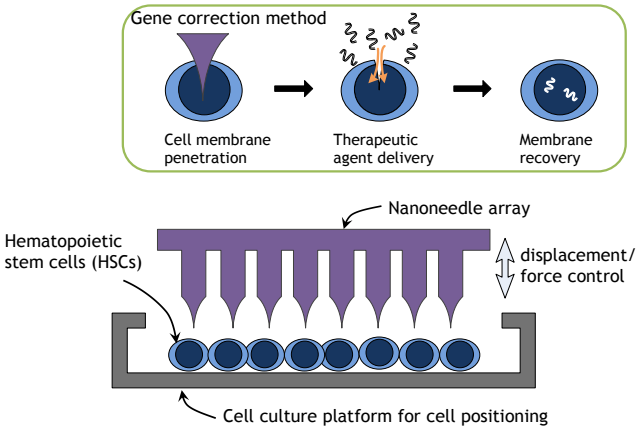

Figure 1: Schematic diagram of intracellular delivery system for insertion of therapeutic genes.

FABRICATION

Fabrication proceeds by patterning a positive photoresist mask (SC1813, Shipley) on a silicon wafer bearing 0.7 micron of thermal oxide. After oxide etching, isotropic dry etching of Si with an SF_6 plasma is performed in order to achieve sharp tips utilizing under-etching of silicon under the etch mask (Figs 2a and 2b). Arrays of circular patterns of 7µm-diameter remain attached to the silicon substrate after the isotropic etching, so that the circular pattern can act as an etch mask during the subsequent anisotropic etching process (Fig. 2c). Due to the directivity from a DC bias during the isotropic etch step [5], a silicon neck region is formed several microns below the mask. After removing residual masks and cleaning, nano-scale silicon tips are formed using an oxidation sharpening process [6] (Fig. 2e). The nanoneedle array is separated into individual 5mm×5mm die and the remaining SiO_2 is removed using HF (Fig. 2f). Figure 3 shows formation of silicon nano-tips after growth of 0.8µm-thick thermal oxide. Figures 3(a) and 3(b) show SEM micrographs of structures during the fabrication process corresponding to the fabrication steps shown in Figures 2(d) and 2(f), respectively.

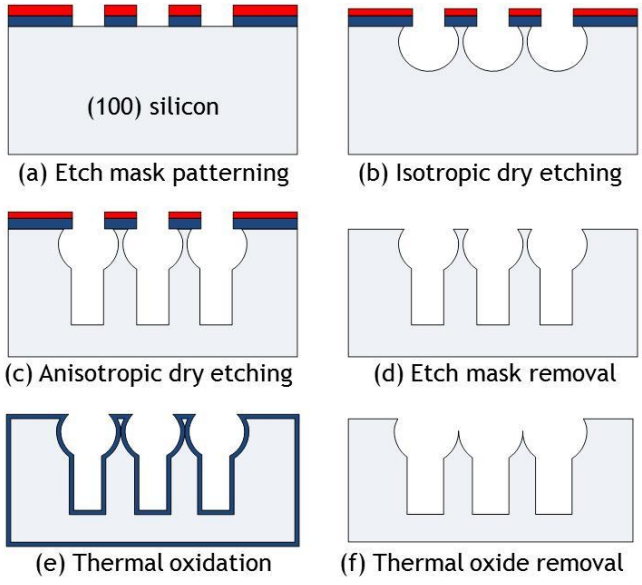

Figure 2: Fabrication process for highly dense silicon nanoneedles (photoresist in red and SiO_2 in blue).

In addition to circular patterns, arrays of regular hexagons and squares were also investigated as etch mask patterns. The sizes of hexagons and squares are determined to inscribe 7μm-diameter circles. The pitch of the patterns is designed to be 10μm, which is close to the typical diameter of cells of interest. In order to achieve regular feature pitch, the circular and hexagonal patterns are arranged in a honeycomb shape as shown in the left side of Figure 4. The square patterns are arranged in a waffle pattern due to the geometric limit of the diagonal length of square patterns.

The profile dependence of nano-tips on the initial shapes of the patterns is shown in Figure 4. The nano-tips were fabricated by using isotropic etching and thermal-oxidation-sharpening processes. The center pictures show an overall view of the tips of circular, hexagonal and square patterns, respectively. The pictures on the right side show a detailed view of the tips, showing tens of nanometers of tip diameter independent of initial shape. Since the micro loading effect during isotropic etching affects the tip profile, gaps between patterns are supposed to be uniform; however, because of a photomask irregularity in the hexagonal patterns, the gaps between vertical edges are wider than those of diagonal edges by a few hundred nanometers. This sub-micron error creates a different etch depth under the mask, resulting in the formation of blades instead of tips. The two insets of Figure 4(b) show orthogonal views of the fabricated nanoneedles, illustrating the blades.

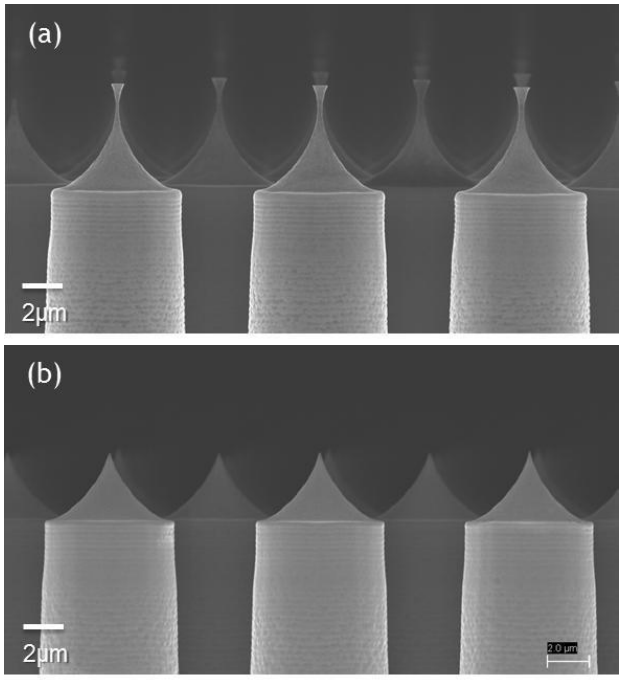

Figure 3: Formation of sharp tips using thermal oxidation. (a) Before oxidation and (b) after oxidation and removal of oxide layer.

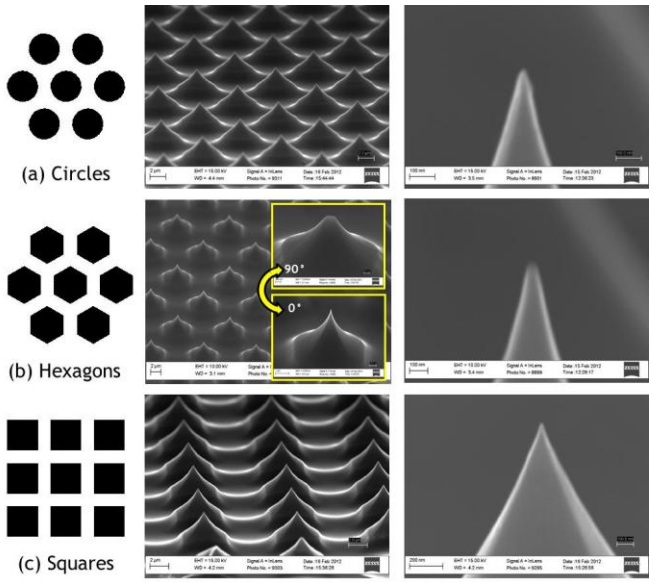

Figure 4: Fabricated nano-tips based on three shapes of mask patterns.

Figure 5 shows individualized nanoneedle arrays separated into 5mm×5mm die, and corresponding SEM micrographs. The height, width and pitch of the nanoneedles are 28μm, 7μm, and 10μm, respectively. The radius of a nanoneedle tip is approximately 16nm. In the experiments described below, nanoneedles fabricated from circular patterns were utilized.

INTRACELLULAR DELIVERY

Materials and methods

As a model cell line, confluent monolayers of human prostate cancer cells (DU145) are cultured in dishes containing a culture medium solution. A calcein fluorescent dye and a fluorescein isothiocyanate labeled bovine serum albumin (FITC-BSA) are used as model molecules that normally do not cross intact cell membranes. The molecular weight and radius of calcein are 623Da and 0.6nm, and those of BSA are 66kDa and 3.6nm, respectively[7].

The backside of a nanoneedle array die is attached to a customized poly(methyl methacrylate) (PMMA) column with base dimension comparable to the die. A substrate bearing cancer cells is immersed in culture medium containing calcein fluorescent dye. The PMMA column bearing the nanoneedle array is placed into contact with the cell-bearing substrate and manually pressed into the cells for 10 s. After removal of the nanoneedles, the cells are left quiescent for 5 min to recover from penetration, and are washed in saline. A propidium iodide (PI) dye is applied onto the cells after the nanoneedle treatment to stain cells killed possibly by needle

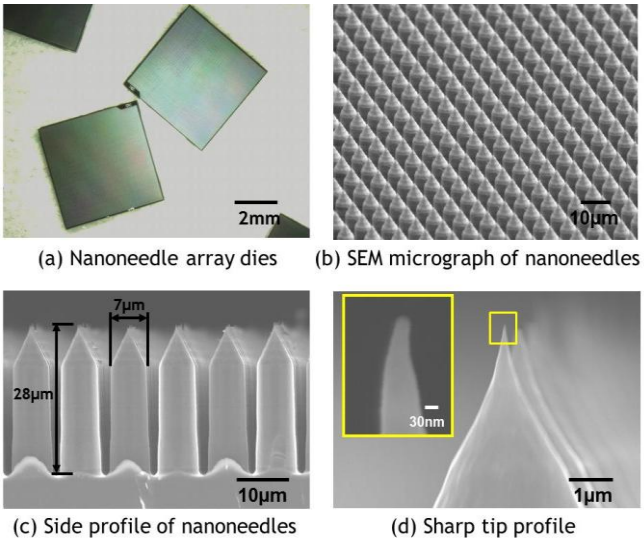

Figure 5: Fabricated 5mm×5mm nanoneedle array with the tip density of $10^6/cm^2$. The radius of a tip is approximately 16nm.

penetration and then washed with saline. This protocol of cell treatment results in the nanoneedle treated cells showing better uptake of calcein than the control group with no significant increase of cell death as shown in Figure 6. Nonetheless, leveling between the attached nanoneedle array and mono-layered cells and uniform application of force were challenging, causing significant variability.

Several protocol changes were implemented to improve the uniformity and reproducibility of the experiment. It was observed that the bare silicon surface is relatively hydrophobic and the nano-patterned silicon is even more so. Direct placement of a nanoneedle array onto cells in solution may trap air, preventing good contact between the nanoneedles and cells. Wetting the surface of the arrays prior to cell contact could alleviate this issue. A droplet of the culture medium solution containing calcein is therefore introduced to the surface of the nanoneedle array, covering the array without overflowing, prior to insertion. The wetted array is then placed in contact with a substrate bearing cells as above. To improve reproducibility of the needle-cell interaction force, a known constant force (1.24g·f, approximately 12mN) was placed on top of the needle array instead of the previously-used manual pressure technique to generate a uniform downward needle-to-cell force. The nanoneedle array was kept in place for 1 min. To reproducibly remove the array, a previously-attached double-sided adhesive tape placed under the weight was utilized as a convenient lifting point. The freestanding weight combined with pre-application of calcein-bearing solution to the array assists self-leveling of the nanoneedle array and enables the application of uniformly-distributed force to the cells. After removing the nanoneedles, the cells are left quiescent for 10 min to allow diffusion of probe molecules and to recover from penetration, followed by a saline wash as described above.

Numbers of cells from control, nanoneedle and bare silicon groups respectively are counted by adopting the ruler method of a hemocytometer. Since a confluent monolayer of cells is grown on the substrate and the field of view of a fluorescent microscope is limited to 3.5mm^2, the center grid of the hemocytometer is sufficient for counting. Therefore cells in five regions of 0.2mm×0.2mm area within a 1mm×1mm square are counted.

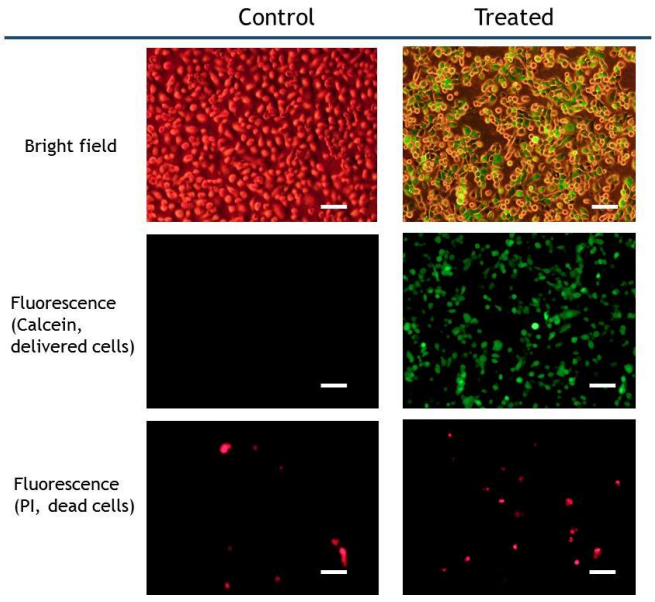

Figure 6: Intracellular delivery test and cell death assay with nanoneedles to DU145 cells (scale bar; 100μm).

Results and discussion

As a preliminary result, nanoneedle-treated cells show intracellular uptake of a small model probe (calcein dye) as shown in Figure 6. The number of treated cells that expresses green color in this field of view is over 70% while the control shows no uptake. However, as mentioned before, leveling issue and non-uniformity of applied force result in a lack of repeatability.

Given a precise control of force application and uniformity, three groups of cells are treated with no die (negative control), nanoneedle die (experiment) and bare silicon die (negative control), respectively. Figure 7 shows representative pictures of a silicon die group and a nanoneedle die group after treatment. In the silicon die case, most of the cells originally on the cell culture substrate were transferred onto the silicon die, leaving a few cells with delivered dye on the original substrate. Most of the cells in the nanoneedle die case, however, remain on the original substrate, resulting in an approximate 30% delivery ratio. Note that the narrow "L" shaped cell-empty region in the bottom center picture is caused by an extruded frame surrounding the nanoneedle die, which is higher than nanoneedles by a few microns due to the nature of the oxidation sharpening process.

Figure 8 summarizes the results of three groups. After each treatment, most of the cells in the no-die control group and the nanoneedle die group remain attached on their original substrates, whereas approximately half of the cells in the silicon die control group are detached from their original substrates. In the silicon die control group, among those cells still adhering to their original substrate, an almost negligible dye uptake as low as 4% of cells was observed, along with 1.5% of cell death. The nanoneedle group shows the highest uptake of the probe molecule up to 34%, while the no-die control group shows no uptake. According to the PI staining, there was no significant difference in cell death between control and nanoneedle application.

To investigate intracellular introduction of larger molecules, a nanoneedle array which has tips fabricated from square patterns without trenches, with height of 3μm, was applied. The techniques of the wetting of the nanoneedle array with the culture medium solution and the application of the constant force containing BSA was applied as above. Since calcein is delivered into cells more easily than macromolecules (i.e. BSA) [7], however, the waiting time for diffusion after the treatment was increased to 40 min. The intracellular uptake of the FITC-BSA by nanoneedles is shown in Figure 9. The nanoneedle technique enables BSA macromolecules to cross the cell membrane and enter the intracellular space.

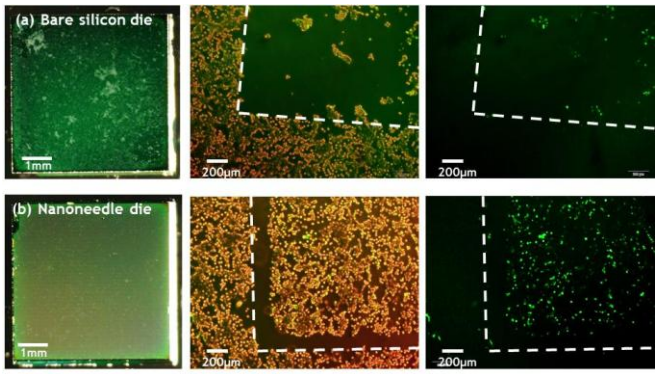

Figure 7: Photographs of dies and treated cells after intracellular delivery tests with (a) a bare silicon die and (b) a nanoneedle array die. (Left) Top surface of the dies, (center) bright filed pictures of the cell-bearing substrate, and (right) fluorescent pictures. White dashed lines mean boundaries of treated area by each die.

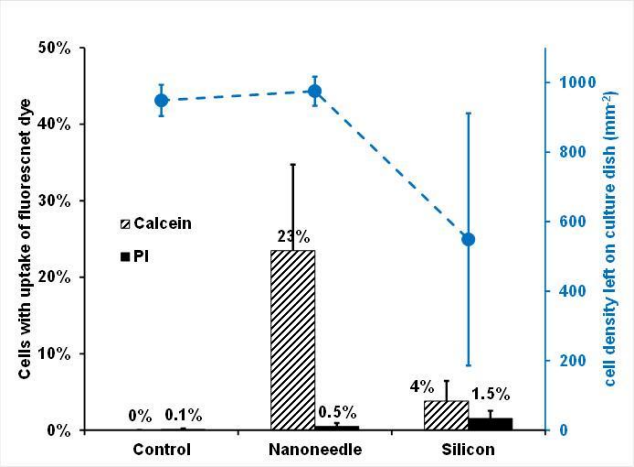

Figure 8: Percent of cell numbers expressing fluorescent light on the substrate after nanoneedle treatment. Cell density left on culture substrates drops significantly after bare silicon treatment. (error bars: standard deviation)

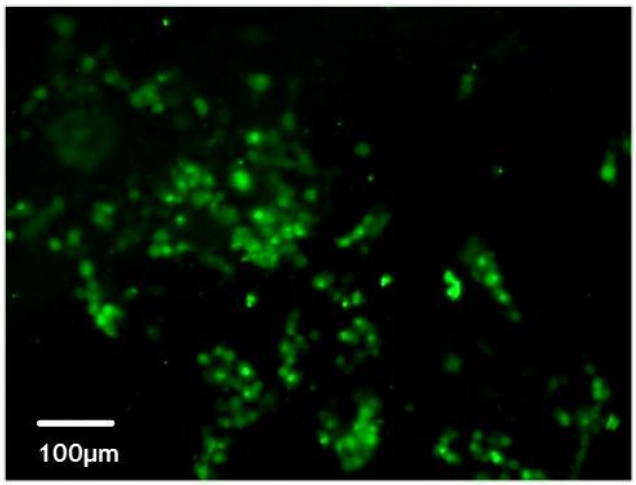

Figure 9: Fluorescent image of cells after BSA delivery with a nanoneedle array

CONCLUSION

By exploiting conventional isotropic etching and a thermal-oxidation-based sharpening process, high-density nanoneedle arrays were produced. The nanoneedles possessed sharp tips as small as 16nm in radius and a high density as large as 10^6 per square centimeters regardless of shapes of mask patterns as long as opening gaps between array elements were consistent. The silicon-micromachined nanoneedles were able to deliver small molecules as well as macromolecules into cells by mechanically penetrating cell membranes. The punctured cells showed uptake of calcein and BSA, respectively, with no significant cell death caused by membrane penetration. The demonstration of intracellular delivery with nanoneedles shows promise for high throughput gene transfer. Additional study on correlation of intracellular uptake of macromolecules with mechanical parameters of nanoneedle treatment for cell membrane penetration, and subsequent demonstration of gene incorporation and expression, is required to further validate this technique.

ACKNOWLEDGMENTS

This work was supported by National Institutes of Health under contract No. 1 PN2 EY018244-01.

REFERENCES

[1] A.K. Shalek, J.T. Robinson, E.S. karp, J.S. Lee, D. Ahn, M. Yoon, A. Sutton, M. Jorgolli, R.S. Gertner, T.S. Gujral, G. MacBeath, E.G.Yang, and H. Park, "Vertical Silicon Nanowires As A Universal Platform For Delivering Biomolecules Into Living Cells", Proceedings of the National Academy of Science, 107, 1870 (2010).

[2] T.I. Pestina, P.W. Hargrove, D. Jay, J.T. Gray, K.M. Boyd, and D. A. Persons, "Correction Of Murine Sickle Cell Disease Using γ-Globin Lentiviral Vectors To Mediate High-Level Expression Of Fetal Hemoglobin", Molecular Therapy, 17, 245 (2009).

[3] K. Chun, G. Hashiguchi, H. Toshiyoshi, H. Fujita, Y. Kikuchi, J. Ishikawa, Y. Murakami, and E. Tamiya, "An Array Of Hollow Microcapillaries For The Controlled Injection Of Genetic Materials Into Animal/Plant Cells", Technical Digest of the 12th IEEE International Conference on Micro Electro Mechanical Systems, Orlando, FL, 1/17-21/99 (1999), pp. 406-411.

[4] K. Chun, G. Hashiguchi, H. Toshioyoshi, B.L. Pioufle, J. Ishikawa, Y. Murakami, E. Tamiya, Y. Kikuchi, and H. Fujita, "DNA Injection Into Plant Cell Conglometrates By Micromachined Hollow Microcapillary Arrays", Technical Digest of the 10th International Conference on Solid-State Sensors and Actuators, Sendai, Japan, 6/7-10/99 (1999), 1B3.2

[5] S.-J. Paik, S. Byun, J.-M. Lim, Y. Park, A. Lee, S. Chung, J. Chang, K. Chun, and D. Cho, "In-Plane Single-Crystal-Silicon Microneedles For Minimally Invasive Microfluid Systems", Sensors and Actuators A: Physical, 114, 276 (2004).

[6] C. Hong and A.I. Akinwande, "Oxidation Sharpening Mechanism For Silicon Tip Formation", Electrochemical and Solid-State Letters, 8, F13 (2005).

[7] H.R. Guzman, D.X. Nguyen, A.J. McNamara, and M.R. Prausnitz, "Equilibrium Loading Of Cells With Macromolecules By Ultrasound: Effects Of Molecular Size And Acoustic Energy", Journal of Pharmaceutical Sciences, 91, 1693 (2002).

CONTACT

*S.-J. Paik, tel: +1-404-894-8807; spaik8@gatech.edu